

# Transport Control by Coherent Zonal Flows in the Core/Edge Transitional Regime

K. Hallatschek and D. Biskamp

*Centre for Interdisciplinary Plasma Science, Max-Planck Institut für Plasmaphysik,  
EURATOM-IPP Association, D-85748 Garching, Germany*

(Received 15 September 2000)

3D Braginskii turbulence simulations show that the energy flux in the core/edge transition region of a tokamak is strongly modulated—locally and on average—by radially propagating, nearly coherent sinusoidal or solitary zonal flows. Their primary drive is the anomalous transport together with the Stringer-Winsor term. The transport modulation and the flow excitation are due to wave-kinetic effects studied for the first time in turbulence simulations. The flow amplitudes and the transport sensitively depend on the magnetic curvature acting on the flows, which can be influenced, e.g., by shaping the plasma cross section.

DOI: 10.1103/PhysRevLett.86.1223

PACS numbers: 52.35.Ra, 52.55.Fa, 52.65.Kj

**Introduction.**—It is now commonly believed that the transport in the tokamak core is controlled by zonal flows [1–3]. In the plasma edge, the flows have not yet been studied thoroughly, but they tend to be weak [4] (although they can possibly completely quench the turbulence [5]). The zonal flows in the core and at the edge were found to be incoherent, random fluctuations [2,6,7]. In contrast to this, in the transitional regime between core and edge, strong radially coherent sinusoidal or solitary zonal flows are ubiquitous according to the numerical simulations described below. The flows in the transitional regime are essentially geodesic acoustic modes (GAM) [8], i.e., the poloidal rotation is coupled to an  $(m, n) = (1, 0)$  pressure perturbation by the inhomogeneous magnetic field, which results in a restoring force and hence an oscillation. Transcending the present models of the zonal flow generation based purely on Reynolds stress [1], the major part of the flow energy in the transitional regime is apparently generated by the Stringer-Winsor (SW) term [9], i.e., the torque on the plasma column caused by the interaction of pressure inhomogeneities with the inhomogeneous magnetic field. The pressure inhomogeneities are driven by anomalous transport modulations, which can be understood by a drift-wave model for the wave-kinetic turbulence response to the flows consistent with additional numerical experiments.

**Zonal flows in the transitional regime are GAMs.**—The numerical turbulence simulations have been carried out using the three-dimensional electrostatic drift Braginskii equations with isothermal electrons, including the ion temperature fluctuations with the associated polarization drift effects, the resistive (nonadiabatic) parallel electron response, and the parallel sound waves (a subset of the equations of Ref. [5]). The nondimensional parameters have been varied around a reference parameter set in the transitional core/edge regime:  $\alpha_d = 0.6$ ,  $\epsilon_n = 0.08$ ,  $q = 3.1$ ,  $\tau = 1$ ,  $\eta_i = 3$ , and  $\hat{s} = 1$ . The computational domain is a flux tube winding around the tokamak for three poloidal connection lengths. The radial and poloidal domain width is  $50L_{RB}$ , with the resistive ballooning scale length,  $L_{RB}$ . For a definition of these parameters and

units see Ref. [5].) The parameters are consistent with the physical parameters  $R = 3$  m,  $a = 1.5$  m,  $L_n = 12$  cm,  $n = 3.5 \times 10^{19} \text{ m}^{-3}$ ,  $Z_{\text{eff}} = 4$ ,  $B_0 = 3.5$  T, and  $T = 300$  eV,  $L_{RB} = 3.6$  mm,  $\rho_s = 0.82$  mm,  $\nu^* = 11$ . At these parameters the ion temperature gradient mode turbulence is the dominant cause of the heat flux [4], and the use of a flux tube domain is justified [7].

Viewed as a function of radius and time, the flux surface averaged poloidal  $\mathbf{E} \times \mathbf{B}$  flows [Fig. 1(a)] start as an irregular pattern of radially propagating independent flows and finally merge into a coherent standing wave. It consists of GAM oscillations, which can be described by suitable Fourier components of the vorticity and pressure equations (neglecting the parallel sound wave),

$$\partial_t \langle v_E \rangle - \langle s_v \rangle = -C_1 \langle p \sin \theta \rangle, \quad (1)$$

$$\partial_t \langle p \sin \theta \rangle - \langle s_p \sin \theta \rangle = C_2 \frac{\epsilon_n}{3} \frac{3 + 5\tau}{1 + \tau} \langle v_E \sin^2 \theta \rangle, \quad (2)$$

with the flux surface average  $\langle \cdot \rangle$ , the pressure fluctuations  $p = n + \frac{\tau}{1+\tau} T_i$ , the poloidal flow velocity  $v_E = \partial_x \phi$ , and the source terms  $s_v/s_p$  of flow/pressure due to Reynolds stress/anomalous transport, respectively. For reference, the two different curvature terms in the equations have been adorned with the factors  $C_1$  and  $C_2$ , which are both 1 in the turbulence equations for a low aspect ratio circular tokamak. The curvature term  $C_1$  is the SW term, the term  $C_2$  represents the up-down asymmetric compression of the plasma due to the poloidal rotation. In the simulations, the zonal flows oscillate with a frequency within 5% of the eigenfrequency of Eqs. (1) and (2) without source terms and with the approximation  $\langle v_E \sin^2 \theta \rangle \approx \langle v_E \rangle / 2$ ,

$$\omega = \sqrt{C_1 C_2 \frac{\epsilon_n}{6} \frac{3 + 5\tau}{1 + \tau}}. \quad (3)$$

In physical units this is  $\sqrt{(6 + 10\tau)/(3 + 3\tau)} c_s / R \sim c_s / R$ . Since the parallel sound frequency  $c_s / (qR)$  is much lower than the GAM frequency, the neglect of the parallel sound wave is justified. The energy balance equation of the GAM oscillations is, according to (1) and (2),

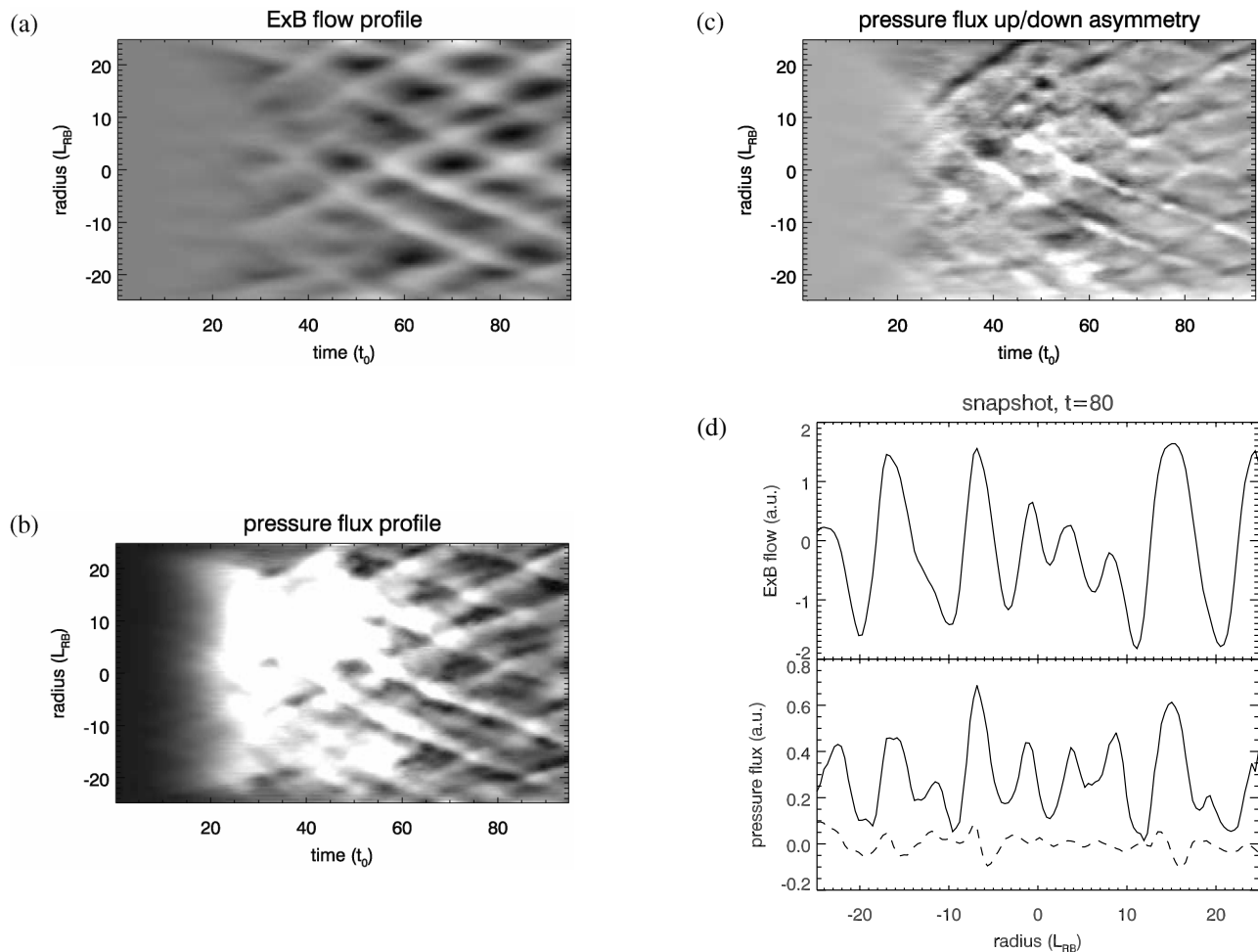


FIG. 1. Time evolution of (a) poloidal  $\mathbf{E} \times \mathbf{B}$  flow profile, (b) pressure flux profile  $\langle v_r p \rangle$ , (c) up-down asymmetric pressure flux  $\langle v_r p \sin \theta \rangle$  for the standard parameters, and (d) instantaneous profiles at  $t = 80$  of the flow (top panel), pressure flux (solid line, bottom panel), and the up-down asymmetric pressure flux (dashed line, bottom panel).  $t_0$  is the turbulence time scale  $\sqrt{RL_n/(2c_s)^2}$ .

$$\partial_t \frac{1}{2} \left[ \langle v_E \rangle^2 + \left( \frac{C_1}{\omega} \right)^2 \langle p \sin \theta \rangle^2 \right] = \langle v_E \rangle \langle s_v \rangle + \left( \frac{C_1}{\omega} \right)^2 \times \langle p \sin \theta \rangle \langle s_p \sin \theta \rangle. \quad (4)$$

In the numerical studies, the energy in the (1,0) pressure perturbations agrees within 20% with the flow energy, confirming that the contributions from stationary flows are irrelevant compared with the GAMs.

The average contributions to the GAM energy from the Reynolds stress term  $\langle s_v \rangle$  and the anomalous transport  $\langle s_p \sin \theta \rangle$  are listed in Table I for varying turbulence parameters. In the transitional regime with its strong coherent zonal flows most of the flow energy is generated by the anomalous transport via the SW term, while with decreasing temperature toward the very edge this SW energy input eventually becomes negative, indicating a braking force on the flows, while simultaneously we get weak incoherent flows. One is tempted to attribute the decrease of the zonal flows towards the very edge to the SW term. Indeed, eliminating the source term  $\langle s_p \sin \theta \rangle$

due to the anomalous transport in the numerical simulations (line marked with \*) leads to relatively strong coherent flows even for parameters in the very edge.

With the natural drive of the GAM being apparently the SW term, it has been found that altering the amplitude of the curvature terms  $C_1, C_2$  acting on the flows, but keeping the curvature terms acting on the turbulence modes fixed, changes the flow amplitudes and the anomalous transport by 1 order of magnitude. Empirically, the flow level rises with increasing  $C_1$  and decreasing  $\omega$ . One reason is that the higher  $(C_1/\omega)^2 \sim C_1/C_2$  is, the higher is the contribution of the anomalous transport source term  $s_p$  to the flow energy (4). At constant ratio  $C_1/\omega$  the flows are still somewhat increasing for decreasing  $\omega$ . This is understood since with an increasing oscillation period the flows have more time to influence the turbulence, resulting in a stronger transport modulation [2] and more efficient flow drive.

The cause of the pressure perturbations driving the flows are local modulations of the anomalous transport (the usual Stringer spin-up mechanism is ineffective due to the relatively long sound transit time in the considered

TABLE I. Mean GAM energy production during the saturation phase due to Reynolds stress and anomalous transport in conjunction with the SW effect, flow intensity  $\langle v_E^2 \rangle$ , and anomalous pressure transport  $\langle p v_r \rangle$  for the reference parameters given in the text, except for varying temperature  $T_i = T_e = T$ . Dimensionless quantities are given in the units of Ref. [5] with  $\alpha_d$  being the diamagnetic drift velocity. Lines with  $\alpha_d = 0$ : ions assumed cold. Line marked with \*: SW drive switched off.

$\alpha_d$	$\eta_i$	$T$ (eV)	$\langle p v_r \rangle$	$\langle v_E^2 \rangle$	Reynolds drive	SW drive
0	—	0	0.27	0.04	1.4	−1.0
0*	—	0	0.25	0.2	3.3	−26
0.2	1	100	0.27	0.03	2.0	−1.0
0.2	3	100	0.87	0.23	1.5	3.6
0.6	3	300	0.15	0.9	−0.1	10.0
1.1	3	550	0.24	0.9	16.0	33.4

regime). Plots of the radial pressure transport  $\langle v_r p \rangle = Q(r, t)$  and its up-down antisymmetric component  $\langle v_r p \sin \theta \rangle = U(r, t)$  are shown in Figs. 1(b) and 1(c). (Note that the pressure source term is the divergence of the anomalous pressure flux, i.e.,  $s_p = -\partial_r(v_r p)$ , and  $\langle s_p \sin \theta \rangle = -\partial_r U$ .) In the initial phase of flow generation,  $U$  develops dipole layers around the flows [Fig. 1(d), dashed line, e.g., at  $x = -7$ ], in which  $U$  always has the same sign as the local shearing rate. These dipolar transport structures generate the pressure up-down asymmetries driving the GAMs. As soon as sufficiently strong flows exist, the anomalous transport  $Q$  develops a striking peaking at the radii of positive flow resembling transport fronts propagating with the flow “waves.” In addition to the dipole structures,  $U$  develops a unipolar part component [dark or bright diagonal streaks in Fig. 1(c)], whose sign depends on the propagation direction of the corresponding flow. These up-down antisymmetric transport fronts can be viewed as avalanches running outward on the lower half of the torus ( $\theta < 0$ ) and inward on the upper half.

The unipolar up-down asymmetries have been found to be responsible for the setup of the flow pattern. If in a numerical experiment the GAMs are initially set to zero outside one flow peak, the turbulence is still capable of moving this flow into the original direction, until a new

standing wave pattern has been formed. The necessary radial GAM energy flow due to the turbulence has been found to be primarily caused by the unipolar up-down asymmetries. Similar events happen, if a numerical simulation is started with a GAM pattern with the wrong wavelength from a simulation run with different GAM parameters. In that case, strong unipolar up-down transport asymmetries develop, which enforce the equilibrium flow propagation velocity, i.e., flow wavelength.

The described peculiar transport modulation is absent for weak diamagnetic drift and vanishing gyro radius, such as in the resistive ballooning regime [4]. Instead, the shear flows simply weaken the turbulence. Besides, the turbulence tends to flatten pressure gradients, i.e., to eliminate the pressure fluctuations associated with the GAM, resulting in the observed braking force.

*The wave-kinetic effects.*—The dependence of the transport modulation on drift effects and the gyro radius suggests a simplified drift-wave model containing only the radial mode coupling due to the polarization drift, eliminating two fluid and curvature effects. Since in the numerical studies the mode wavelengths are not small compared to the zonal flow scales, we refrain from a geometrical optics approach [1] and instead move back to the linearized adiabatic drift-wave equation,

$$D_t(1 - \rho_s^2 \Delta_\perp) \phi + \alpha_d \partial_y \phi = 0, \quad (5)$$

with  $D_t = \partial_t + v_E(x, t) \partial_y$ , the ion sound Larmor radius  $\rho_s$ , and the drift velocity  $\alpha_d$ . We study the impact of the polarization drift term  $-D_t \rho_s^2 \Delta_\perp n$  up to first order in  $\rho_s^2$ , without assumptions on the ratio of flow vs turbulence scales. The zeroth order time evolution (with  $y$  in Fourier space) is

$$\phi_0(x, t) = \phi_i(x) \psi(x, t) \quad (6)$$

with initial amplitude  $\phi_i(x)$  and the flow-and-drift induced phase factor

$$\psi(x, t) = \exp[-ik_y \xi], \quad \xi = \int_0^t [v_E(x, \tau) + \alpha_d] d\tau. \quad (7)$$

Inserting (6) into (5) results in the first order correction  $\phi_1$  due to  $\rho_s^2$ ,

$$\phi_1(x, t) \psi^*(x, t) = -ik_y \alpha_d \rho_s^2 \int_0^t \psi^*(x, \tau) \Delta_\perp (\phi_i \psi(x, \tau)) d\tau + \rho_s^2 [\psi^*(x, \tau) \partial_x^2 (\phi_i \psi(x, \tau))]_{\tau=0}^{\tau=t}, \quad (8)$$

in which  $[f(\dots, \tau)]_{\tau=0}^{\tau=t} \equiv f(\dots, t) - f(\dots, 0)$ . From this, the change in turbulence intensity can be computed to first order,

$$\delta |\phi|^2 = 2 \operatorname{Re}(\phi_1^* \phi_0) = 2k_y \alpha_d \rho_s^2 \int_0^t \partial_x [k_x(x, \tau) |\phi_i|^2] d\tau - 2\rho_s^2 [k_x^2(t) - k_x^2(0)] |\phi_i|^2, \quad (9)$$

with a suitable local  $k_x(x, \tau) \equiv -k_y \xi'(x, \tau) + \operatorname{Im}(\phi_i' / \phi_i)$ . The term involving the diamagnetic drift velocity  $\alpha_d$  corresponds to the advection of mode intensity in response to the shearing distortion, while the other term is analogous to the adiabatic compression of a wave field.

If the initial  $\phi_i$  has no radial structure ( $k_x = 0$ ) and the shear flows do not change with time, we obtain, due to radial mode advection,

$$\delta |\phi|_{\text{advection}}^2 = -\rho_s^2 \alpha_d |\phi_i|^2 t^2 k_y^2 v_E'', \quad (10)$$

which explains the empirical peaking in turbulence intensity at the locations of positive flows. To verify the presence of the advection term, a complementary scenario has been simulated, with the turbulence initially confined to small regions and a constant linear shear flow  $v_E \propto x$  enforced upon it. This results in a motion of the turbulence

maxima towards increasing  $v_E$ , which confirms the presence of the advection term (see Fig. 2). In another numerical experiment, a stationary bell-shaped flow profile has been superposed on an initially radially homogeneous turbulence field, which has been prepared with the zonal flows switched off. After the turbulence rises transiently at the flow maximum, it drops to a level below the initial one. This corroborates that the turbulence amplification at the flow maxima is not due to an increase of drive at the flow maxima [10], but is due to a transient wave-kinetic concentration of fluctuation energy.

The numerically observed radial dipole layers of up-down antisymmetric transport apparently result from the compressional terms in (9) acting on the mode structure enforced by the magnetic shear, namely,

$$k_x \sim k_y \hat{s} \theta. \quad (11)$$

Hence, with  $\hat{s} = 1$ , a shear flow with positive  $v'_e$  reduces  $k_x^2$  on the upper side of the tokamak ( $\theta > 0$ ), increasing the mode amplitude there, while the mode is attenuated for ( $\theta < 0$ ). The dependence of this effect on the magnetic shear has been verified in a numerical experiment with  $\hat{s} = -1$ , in which the modes are amplified for  $\theta v'_e < 0$ . Moreover, a “swinging through” effect has been observed, i.e., the turbulence intensity decreases again when  $k_x^2$  rises after  $k_x$  has gone through zero.

Last, we consider the unipolar up-down transport asymmetries induced by a propagating positive shear flow (which is accompanied by a general transport peaking due to the advective effect). With  $v_E(x, t) = V(x - \nu t)$  (propagation velocity  $\nu$ ) we obtain, from definition (7),  $\xi'(x, t) = -\nu^{-1} V(x - \nu t)$ , i.e.,

$$k_x(x, t)^2 = (k_{x0} - k_y \xi')^2 = k_y^2 [\hat{s} \theta + \nu^{-1} V(x - \nu t)]^2. \quad (12)$$

A reduction of  $k_x^2$  and the corresponding amplification of the turbulence modes via Eq. (9) occur for  $\hat{s} \theta \nu V < 0$ . The sign of this effect of a moving flow has been confirmed numerically for positive and negative shear.

**Conclusions.**—GAMs, oscillating zonal flows, control the turbulence level in the transitional core/edge regime. Primarily, they are not driven by Reynolds stress but by the pressure asymmetries on a flux surface generated by anomalous transport modulations. The flows in turn cause the transport modulations, on one hand, by concentrating the turbulence in regions of increased flow in electron diamagnetic direction due to the radial mode drifts, and, on the other hand, by adiabatic compression of the wave field, which together with the magnetic shear result in an up-down asymmetric transport. Both wave-kinetic effects have been studied separately in numerical experiments. Together, they lead to propagating peaked flow structures accompanied by pronounced transport fronts, sometimes coming close to solitons. Similar results should be expected for the core, except that the polarization due to the ion Larmor radius has to be replaced by the neoclassi-

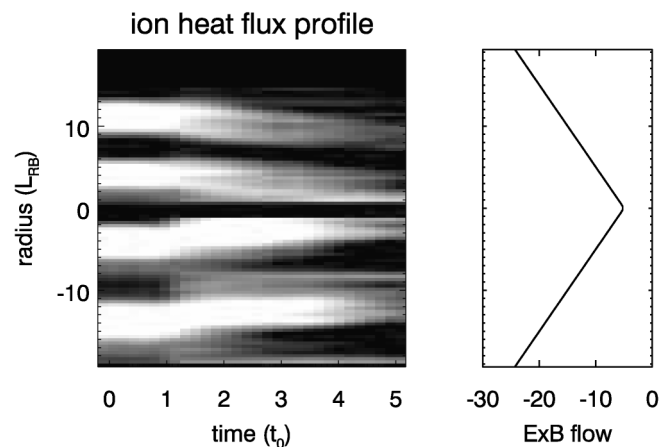


FIG. 2. Time evolution of heat flux profile in response to linear shear flow with different signs for upper and lower halves.

cal polarization due to the banana width [11] boosting the wave-kinetic transport modulation. GAMs are less important in the core due to the short parallel connection length ( $q \sim 1$ ).

On one hand, the GAM drive efficiency depends on the nature of the turbulence; e.g., absence of finite  $\rho_s$  and drift effects, such as in the resistive ballooning regime, leads to a strong flow damping due to the anomalous diffusion eroding the pressure fluctuations connected with the GAM. On the other hand, manipulation of the linear properties of the GAM itself, such as its frequency or the torque exerted on a pressure fluctuation, can lead to a reduction of the transport by up to an order of magnitude. Consequently, any discussion of the anomalous transport focusing on the influence of the magnetic geometry on the turbulence drive but neglecting its influence on the flows misses an essential factor. Since the GAM properties depend, e.g., on the shape of the plasma column, the coherent flows should be taken into consideration to further reduce the transport in advanced tokamaks. Moreover, the clear signature of the radially coherent flows in the numerical simulations makes them an interesting target of experimental investigation [12], e.g., by means of microwave reflectometry.

- 
- [1] P.H. Diamond *et al.*, Proceedings of the 17th IAEA Fusion Energy Conference, Report No. IAEA-CN-69/TH3/1, 1998.
  - [2] T.S. Hahm *et al.*, Phys. Plasmas **6**, 922 (1999).
  - [3] P.W. Terry, Rev. Mod. Phys. **72**, 109 (2000).
  - [4] A. Zeiler *et al.*, Phys. Plasmas **5**, 2654 (1998).
  - [5] B.N. Rogers *et al.*, Phys. Rev. Lett. **81**, 4396 (1998).
  - [6] Z. Lin *et al.*, Phys. Plasmas **7**, 1857 (2000).
  - [7] K. Hallatschek, Phys. Rev. Lett. **84**, 5145 (2000).
  - [8] S.V. Novakovskii *et al.*, Phys. Plasmas **4**, 4272 (1997).
  - [9] A.B. Hassam *et al.*, Phys. Plasmas **1**, 337 (1994).
  - [10] K.L. Sidikman *et al.*, Phys. Plasmas **1**, 1142 (1994).
  - [11] M.N. Rosenbluth *et al.*, Phys. Rev. Lett. **80**, 724 (1998).
  - [12] T.S. Hahm *et al.*, Plasma Phys. Controlled Fusion **42**, A205 (2000).